U.S. ARMY COMBAT CAPABILITIES DEVELOPMENT COMMAND
CHEMICAL BIOLOGICAL CENTER

ABERDEEN PROVING GROUND, MD 21010-5424

CCDC CBC-TR-1617

Accurate Evaluation of Potential Calibration Standards for Ion Mobility Spectrometry

Brian C. Hauck
Charles S. Harden

SCIENCE AND TECHNOLOGY CORPORATION
Belcamp, MD 21017-1427

Vincent M. McHugh

RESEARCH AND TECHNOLOGY DIRECTORATE

February 2020

Disclaimer

The findings in this report are not to be construed as an official Department of the Army position unless so designated by other authorizing documents.

REPORT DOCUMENTATION PAGE

Form Approved
OMB No. 0704-0188

1. REPORT DATE *(DD-MM-YYYY)*	2. REPORT TYPE	3. DATES COVERED *(From - To)*
XX-02-2020	Final	May 2017–Jun 2018

4. TITLE AND SUBTITLE
Accurate Evaluation of Potential Calibration Standards for Ion Mobility Spectrometry

5a. CONTRACT NUMBER

5b. GRANT NUMBER

5c. PROGRAM ELEMENT NUMBER
63004/L97

6. AUTHOR(S)
Hauck, Brian C.; Harden, Charles S. (STC); and McHugh, Vincent M. (CCDC CBC)

5d. PROJECT NUMBER

5e. TASK NUMBER
04

5f. WORK UNIT NUMBER

7. PERFORMING ORGANIZATION NAME(S) AND ADDRESS(ES)
Science and Technology Corporation (STC); 111 C. Bata Blvd., Belcamp, MD 21017-1427
Director, CCDC CBC, ATTN: FCDD-CBR-ID, APG, MD 21010-5424

8. PERFORMING ORGANIZATION REPORT NUMBER
CCDC CBC-TR-1617

9. SPONSORING / MONITORING AGENCY NAME(S) AND ADDRESS(ES)
Joint Project Manager for Nuclear, Biological and Chemical Contamination Avoidance, APG, MD 21010-5424

10. SPONSOR/MONITOR'S ACRONYM(S)
JPM NBC CA

11. SPONSOR/MONITOR'S REPORT NUMBER(S)

12. DISTRIBUTION / AVAILABILITY STATEMENT
Approved for public release: distribution unlimited.

13. SUPPLEMENTARY NOTES
U.S. Army Combat Capabilities Development Command Chemical Biological Center (CCDC CBC) was previously known as U.S. Army Edgewood Chemical Biological Center (ECBC).

14. ABSTRACT: (Limit 200 words)
Ion mobility spectrometry (IMS)-based instruments have historically been accurate to, at best, ±2% of the reduced ion mobility (K_0) value of the chemical of interest. Fielded IMS-based detectors that are in use for hazardous and illicit substance detection are subject to false-positive alarms because of this inaccuracy and the resulting wide alarm windows, which are required to maintain a high rate of true-positive alarms. To reduce false-positive alarm rates and improve the accuracy of any IMS-based instrument, accurate K_0 values of an ion mobility reference standard need to be used for ion mobility scale calibration. However, a suitable calibrant has yet to be accurately analyzed and agreed upon by the IMS community. In this study, we have chosen five potential IMS calibrants on the basis of their rating against seven criteria for suitable standards and analyzed them as a function of drift gas temperature and humidity using an accurate ion mobility instrument. Recommendations are made herein for each potential calibrant's suitability as a standard for the wider IMS community.

15. SUBJECT TERMS

Ion mobility spectrometry (IMS)	Reference standards	Accuracy
Calibration	Reduced ion mobility (K_0)	Accurate ion mobility instrument (AIMI)

16. SECURITY CLASSIFICATION OF:			17. LIMITATION OF ABSTRACT	18. NUMBER OF PAGES	19a. NAME OF RESPONSIBLE PERSON
a. REPORT	b. ABSTRACT	c. THIS PAGE			Renu B. Rastogi
U	U	U	UU	36	19b. TELEPHONE NUMBER *(include area code)* (410) 436-7545

Blank

PREFACE

The work described in this report was authorized under the Army Technology Objective, "Detection of Unknown Bulk Explosives," under program 63004/L97, task 04, and the Joint Project Manager for Nuclear, Biological and Chemical Contamination Avoidance (Aberdeen Proving Ground [APG], MD) military interdepartmental purchase request (MIPR) numbers 10864246 and 4550199830. This work was supported, in part, by an appointment to the Internship/Research Participation Program at the U.S. Army Edgewood Chemical Biological Center (ECBC; APG, MD) and administered by the Oak Ridge Institute for Science and Education (Belcamp, MD) through an interagency agreement between the U.S. Department of Energy (Washington, DC) and ECBC. At the time this work was performed, the U.S. Army Combat Capabilities Development Command Chemical Biological Center (CCDC CBC; APG, MD) was known as ECBC. This work was started in May 2017 and completed in June 2018.

The use of either trade or manufacturers' names in this report does not constitute an official endorsement of any commercial products. This report may not be cited for purposes of advertisement.

This report has been approved for public release.

Acknowledgments

The authors acknowledge Dr. Augustus W. Fountain (ECBC, retired) and Jasmine Wilding (ECBC) for their assistance in acquiring funding.

Blank

CONTENTS

FIGURES

TABLES

Blank

ACCURATE EVALUATION OF POTENTIAL CALIBRATION STANDARDS FOR ION MOBILITY SPECTROMETRY

1. INTRODUCTION

Ion mobility spectrometry (IMS) has become the preferred analytical technique for detecting hazardous and illicit substances such as explosives, chemical warfare agents, toxic industrial chemicals, and pharmaceutical-based analogues due to the small size, weight, power, and fast response time of an IMS system. IMS-based devices are used to separate and identify chemicals of interest based on their ions' size-to-charge ratios and resulting reduced ion mobility (K_0) values. An ion's K_0 value is calculated by measuring its drift time (t_d, seconds) under a voltage gradient (V, volts), across a known length (L, centimeters). The temperature (T, kelvin) and pressure (P, torr) of a countercurrent neutral drift gas is then normalized against standard temperature and pressure, as shown in eq 1.[1,2]

$$K_0 = \frac{L^2}{Vt_d}\left(\frac{273.15}{T}\right)\left(\frac{P}{760}\right) \quad (1)$$

For currently fielded IMS-based systems, such as the lightweight chemical detector (LCD 3.3; Smiths Detection; London, U.K.), alarm windows for each chemical of interest are created on the basis of multiple K_0 value measurements from several types of IMS-based detectors under multiple temperature and relative humidity conditions. If a peak appears within an alarm window, an alarm is sounded for the chemical associated with that window. Variations in instrument design, temperature, and pressure can cause variations in the calculation of the K_0 values. As a result, multiple detectors that are under identical conditions and simultaneously exposed to the same chemical will show a range of responses.[3] Detection algorithms are then forced to use relatively wide alarm windows, at best, approximately ±2% of the average K_0 value, to maintain a high rate of true-positive alarms. However, when a non-hazardous interferent appears within them, these detectors are often subject to false-positive alarms because of this sizable alarm window width. Conversely, these windows cannot be arbitrarily narrowed or the rate of false-negative responses to valid chemicals of interest will increase.

Before leaving the factory, each LCD 3.3 system is calibrated by exposing it to di(propylene glycol) methyl ether (DPM) and methyl salicylate (MES) for positive and negative ion calibration, respectively. An individual mobility scale correction factor is applied to each detector based on its response to the calibration standards, and each detector has a slightly different correction factor due to variations among detectors, as previously mentioned. However, the K_0 value of the calibrant used to calculate this factor was based on an inaccurate average of multiple measurements across multiple conditions and detectors. These correction factors need to be updated over time because the detector response drifts out of calibration, and this can only be done by sending the detector back to the factory.[3] The solution to reducing the width of alarm windows for chemicals of interest, and as a result, reducing the false-positive alarm rates of these

detectors, while increasing the the overall accuracy of all IMS-based systems, is to develop and implement an on-demand calibration strategy using high-accuracy reference K_0 values.

The staff at U.S. Army Edgewood Chemical Biological Center (Aberdeen Proving Ground, MD), now known as the U.S. Army Combat Capabilities Development Command Chemical Biological Center have continued to address this issue and have an accurate ion mobility instrument (AIMI) that is capable of measuring K_0 values with an optimized accuracy of ±0.1%, which is an order of magnitude better than previous systems.[4–10] These high-accuracy K_0 values can be used in an on-demand detector calibration strategy as shown in eq 2.

$$K_{0\,\mathrm{det}} = \left(\frac{K_{0\,\mathrm{std}}}{K_{0\,\mathrm{cal}}}\right) K_{0\,\mathrm{obs}} \tag{2}$$

In this calibration strategy, the end user would enter a "calibration mode" on the IMS-based detector and apply a calibrant compound. The detector would be used to measure the uncalibrated K_0 value of the calibrant ($K_{0\,\mathrm{cal}}$), and this value would be compared to the accurate K_0 value of the calibrant ($K_{0\,\mathrm{std}}$) under the same conditions, which was previously determined by the AIMI and stored within an internal library. The ratio of $K_{0\,\mathrm{std}}$ to $K_{0\,\mathrm{cal}}$ is the calibration factor that would be applied to the ion mobility scale and every other inacurate K_0 value that was observed in the spectrum ($K_{0\,\mathrm{obs}}$). The function would then return an accurate K_0 value for identification and alarm purposes ($K_{0\,\mathrm{det}}$).[3] Using $K_{0\,\mathrm{std}}$ in this calibration strategy will increase agreement between detectors and reduce false-positive alarms. A low rate of false-negative responses will be maintained by using accurately measured K_0 values of the chemicals of interest to shift the detection windows to their proper location on the calibrated ion mobility scale on the basis of the instrumental conditions present during detector calibration. Although this strategy has been developed for alarm windows and threat detection scenarios, it is applicable to any drift time IMS-based instrument because the end result is a calibrated ion mobility scale that is traceable to National Institute of Standards and Technology (Gaithersburg, MD) accuracy.[4]

$K_{0\,\mathrm{std}}$ needs to be accurately and precisely defined across the range of operational conditions for the detector to generate the appropriate correction factor at those same conditions. However, an accurate in-depth analysis of potential reference standards does not exist, and as a result, the wider ion mobility community has yet to decide upon a suitable standard chemical for use as a calibrant. We have published a review proposing seven criteria against which chemicals can be evaluated for use as suitable reference standards.[3] Ideally, the calibrant should be easily ionizable, have minimal safety hazards, have a vapor pressure commensurate with the mode of introduction, have a minimal number of possible isomers, have commercial availability in high purity, be active in both positive and negative ion detection modes, and be able to produce both monomer and dimer species.[3] A minimal number of isomers will reduce the range of potential collision cross sections and reduce the potential for unresolved ion mobility peaks associated with each isomer. Commercial availability as a high-purity chemical will allow for the wide dissemination and use of the chemical among the IMS community. Activity in both positive and negative ionization modes will reduce the number of chemicals needed to calibrate the detector. Because the K_0 values of monomer species are often sensitive to changes in the drift gas water content, whereas dimer species K_0 values are typically relatively insensitive and unchanging, the

two can be leveraged to empirically measure the water content of the drift gas inside the drift tube. This will allow for more accurate selection of K_0 values of both the calibrant and chemicals of interest at those same instrumental conditions.[8] In this study, we have rated multiple potential calibrant compounds against the aforementioned criteria, and from that list, we have chosen five chemicals for initial accurate analyses as potential calibrants for IMS systems as follows: 2,4-pentanedione (PDO); 2,6-di-*tert*-butylpyridine (D*t*BP); triethyl phosphate (TEPO); DPM; and MES. Historically, dimethyl methylphosphonate (DMMP) has also been of interest as a calibrant and was previously analyzed.[5] Isoflurane (IsoF) is also a proposed calibrant, but a detailed evaluation of its suitability has not been completed.[11] Herein, we report the accurate K_0 values of these five potential calibrants across the range of operational conditions for the LCD 3.3 system and analyze their suitability as IMS reference standards for the wider IMS community.

2. EXPERIMENTAL SECTION

2.1 Ion Mobility Time-of-Flight Mass Spectrometer (TOFMS)

The AIMI on which accurate K_0 values were measured is a hermetically sealed, stacked-ring design that is capable of measuring the variables in eq 1 to an accuracy of ±0.1%.[4,5] The AIMI drift tube was interfaced to a TOFMS (Ionwerks, Inc.; Houston, TX) to mass identify all ion mobility peaks. A nickel-63 ionization source was used in the negative ion detection mode to avoid the formation of NO_x species when using corona ionization. A corona ionization source was used in the positive ion detection mode and consisted of a 20 kV high-voltage feedthrough (Solid Sealing Technology, Inc.; Watervliet, NY) welded above the central drift gas exit of an Alloy 46 base having the same dimensions as the nickel-63 ionization source. A wire mesh screen that was attached to the first electrode of the drift tube served as the counter electrode, and a separate wire mesh screen mounted to the ionization source base using Macor rods (Corning Inc.; Corning, NY) served to confine the equipotential lines of the drift tube and cover the hole where the nickel-63 foil was previously inserted into the reaction region. Voltage was supplied to the feedthrough by a molded silicone, high-voltage plug (Solid Sealing Technology) and a corona was established by a 50 μm diameter stainless steel wire (McMaster-Carr; Elmhurst, IL) that was wrapped around the opposite end of the feedthrough and insulated from the base by a Macor sleeve.

The length of the drift tube, between two Bradbury–Nielson (BN) ion gates, was 16.249 ± 0.007 cm at room temperature and was corrected for thermal expansion. The electric field intensity of the drift tube was set to 280 V/cm as slight variations in K_0 values occur in the low field domain.[6,7] Ion drift times were calculated as the difference between drift time measurements taken from each BN ion gate operated with a 200 μs pulse width. Temperature gradients within the drift gas were reduced to within ±0.1 °C across the length of the drift tube, and data were collected at 25, 30, 40, and 50 °C. Ambient pressure was measured using a Princo model 453 standard mercurial barometer (Precision Thermometer & Instrument Co.; Philadelphia, PA) and was corrected for temperature and latitude at the measurement point.

2.2 Chemicals and Solvents

All candidate calibrants were obtained from Sigma-Aldrich Chemical Co. (St. Louis, MO). PDO, D*t*BP, TEPO, and MES were obtained as 99, 97, 99.8, and 99% pure standards, respectively. DPM was obtained as a 99% pure standard that consisted of a mixture of four isomers. Certified Trace Source disposable ammonia permeation tubes were used to create a 20 ppm_v drift gas dopant (KIN-TEK Analytical, Inc.; La Marque, TX) under a 1.00 ± 0.01 L/min flow of drift gas supplied by compressed house air (~1 ppm_v H_2O) and an 1179A digital mass flow controller with a 247D power supply and readout (MKS Instruments; Andover, MA). Using these conditions eliminated the water reactant ion peak [$H(H_2O)_n^+$] in favor of an ammonia reactant ion peak [$H(NH_3)_n^+$]. High-performance liquid chromatography (HPLC)-grade water (Fisher Scientific; Hampton, NH) was introduced as a drift gas modifier to simulate humidity effects on K_0 values.

2.3 Water and Dopant Introduction

A silica capillary (150 µm i.d., 360 µm o.d.; Polymicro Technologies; Phoenix, AZ) was inserted into the drift gas line before the mass flow controller and connected to a 250 µL Gastight no. 1725 syringe (Hamilton Co.; Reno, NV) using Valco Instruments Co., Inc. (Houston, TX) fittings. A 74900 series, single-syringe infusion pump (Cole-Parmer Instrument Co.; Vernon Hills, IL) was operated as needed up to 60 µL/h to set desired drift gas water content levels between approximately 5 and 550 ppm_v. During the acquisition of each spectrum, a previously written LabVIEW program (National Instruments; Austin, TX) was used to record drift gas water contents measured by a Moisture Image Series 1 hygrometer and probe (GE Measurement and Control; New Fairfield, CT). Ammonia permeation tubes were inserted in-line with the drift gas after the hygrometer probe. Ammonia dopant was present in the drift and reaction regions of the instrument and in both the positive and negative ion detection modes to simulate field instrument conditions.

2.4 Sample Introduction

Neat liquid sample (1 µL) was pipetted into a 1/4 in. o.d., 2.5 in. long glass ampoule (Glassblowers.com, Inc.; Turnersville, NJ) through a Kovar-to-glass seal. The ampoule was attached to the sample gas line with a 1/4 in. Swagelok nut and Teflon fitting (Solon, OH), and an orthogonal flow of house air carried headspace vapors through a silica capillary (150 µm i.d., 360 µm o.d.) and into the reaction region of the AIMI drift tube via a port in one of the reaction region electrodes.[4] The small diameter capillary minimized any temperature gradients resulting from the introduction of room temperature sample air. When needed, sample was intermittently introduced in short intervals to maintain sufficient product ion peak height. A 15 kV ceramic isolator (Solid Sealing Technology) was used to electrically isolate the drift tube from the sample gas line.

3. RESULTS AND DISCUSSION

3.1 PDO

Although structural isomers for PDO exist, it was selected as a potential ion mobility reference standard for its relatively high vapor pressure (6 mmHg at 20 °C), activity in both positive and negative ion detection modes, and ability to produce both a protonated monomer ion and proton-bound dimer ion under non-ammoniated conditions.[3,7] Because of the lack of steric hindrance around the protonation site, it was assumed that PDO would behave similarly to DMMP and also form ammoniated monomer and dimer species under ammoniated conditions, as an ammoniated monomer ion [$(PDO)NH_4^+$, mass-to-charge ratio (*m/z*) 118] and as an ammonium-bound dimer ion [$(PDO)_2NH_4^+$, *m/z* 218].[5] After introduction into the drift tube, $(PDO)NH_4^+$ was observed in the mass spectrum, but only a small amount of $(PDO)_2NH_4^+$ was observed to be present, even at high vapor concentrations. Bridging was observed across the monomer and dimer peaks in the ion mobility spectrum, which indicated that the dimer decomposed within the drift space in a manner similar to other unstable species; therefore, K_0 values could not be accurately measured.[2,12]

PDO spectra were obtained using an LCD 3.3 system, as shown in Figure 1. The overall spectrum (blue curve) was magnified in the area between drift times of 3 and 9 ms and below a peak amplitude of 2000 (arbitrary units). The concentration of vapors was estimated to be 2000 ppm_v, but the dimer peak height was only approximately 5% of the monomer peak height, and bridging was still observed. In Figure 1, the bridging between peaks is highlighted when individual peaks for the reactant ion (red), PDO monomer ion (yellow), and PDO dimer ion (green) were drawn based on a symmetrical distribution around each peak's maximum. The white space between the overall spectrum and the symmetrically distributed peaks corresponds to the unstable monomers and dimers that decomposed in the drift region. Negative product ions were also observed, but the potential spectrum complications and lack of stable dimer species under ammoniated conditions make PDO an unsuitable ion mobility reference standard.

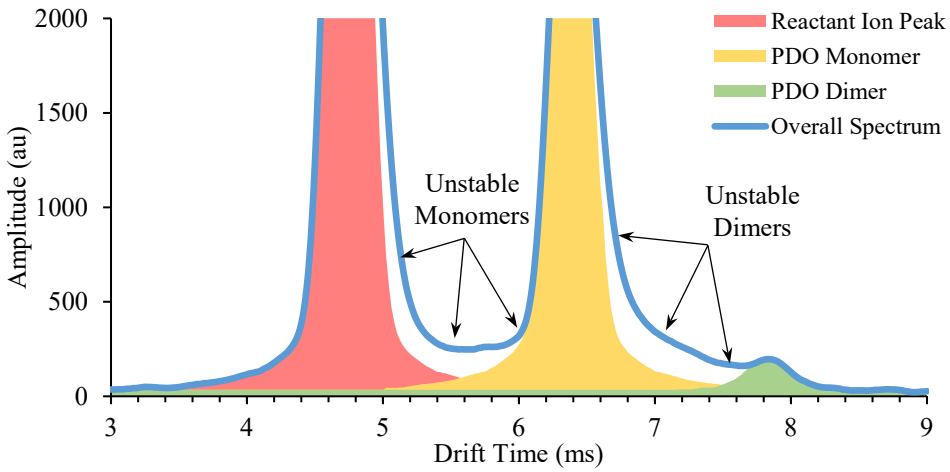

Figure 1. Magnified PDO spectrum on an LCD 3.3 under ammoniated conditions. The overall spectrum (blue) and individual peaks for the reactant ion peak (red), PDO monomer (yellow), and PDO dimer (green) were drawn based on a symmetrical distribution around the peak maxima.

3.2 D*t*BP

D*t*BP has a relatively high vapor pressure (0.177 mmHg at 20 °C), and the K_0 value of its monomer ion is insensitive to changes in temperature and drift gas water content. However, D*t*BP is active only in the positive ion detection mode and does not form dimer species. Structural isomers for the compound exist.[3] D*t*BP was first proposed as an instrumental standard by Eiceman et al., and an estimated K_0 value of 1.42 $cm^2V^{-1}s^{-1}$ has since been used by other researchers for calibration purposes.[5,13,14] When D*t*BP was introduced into the drift tube under ammoniated conditions, a protonated monomer ion of D*t*BP [(D*t*BP)H^+, *m/z* 192] was observed. This indicated that the amine within the molecule was protected by the steric hindrance of the *tert*-butyl group to prevent neutrals like ammonia or water from clustering with it. This was confirmed by Valadbeigi et al., whose thermodynamic calculations did not support the formation of an ammoniated monomer ion of D*t*BP [(D*t*BP)NH_4^+] or the clustering of any waters around the ion. The authors also observed only (D*t*BP)H^+ and an identical drift time under both ammoniated and non-ammoniated conditions at 110 ± 2 °C, 640 V/cm, 0.75 bar (562 Torr), and low humidity (10–50 ppm_v H_2O) zero air as the drift gas.[15] The effect of drift gas temperature and water content on the K_0 value of (D*t*BP)H^+ in the AIMI drift tube is shown in Figure 2.

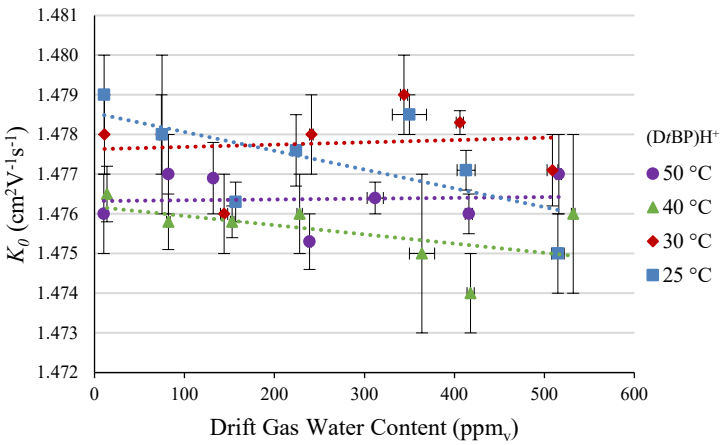

Figure 2. Effect of drift gas water content on the K_0 value of (D*t*BP)H$^+$ at 25.0 ± 0.1 (■), 30.0 ± 0.1 (◆), 40.2 ± 0.1 (▲), and 50.0 ± 0.1 (●) °C.

The overall average K_0 value of (D*t*BP)H$^+$ across the entire range of investigated temperatures and drift gas water contents was 1.477 ± 0.001 cm^{2}V^{-1}s^{-1}. This value was a 4% increase over the traditional value, and the overall range was 1.474 ± 0.001 to 1.479 ± 0.001 cm^{2}V^{-1}s^{-1}. The linear regression coefficient (R^2) value of each temperature's trend line was low at 0.42, 0.01, 0.22, and 0.001 for 25, 30, 40, and 50 °C, respectively, which indicates a minimal dependence of the K_0 value on drift gas water content. This independent scattering of data points around the average value indicates that D*t*BP would make a suitable instrumental standard. If used, the corresponding negative ion detection mode calibrant would need to be one that forms monomer and dimer species to quantify drift gas water content.

3.3 TEPO

The physical properties of TEPO are similar to those of DMMP, which has also been previously considered as an ion mobility standard.[3,5] TEPO has a relatively high vapor pressure (0.1 mmHg at 20 °C), has no structural isomers, and forms monomer and dimer species that could be used to empirically measure drift gas water content. However, it is only active in the positive ion detection mode.[3] There is a lack of published K_0 values for TEPO under ammoniated conditions, and previously published values are typically based on water ion chemistry or when acetone or dimethyl sulfoxide dopants are present.[16,17] Satoh et al. used an LCD 3.3 system to measure the K_0 value of TEPO under ammoniated and ambient temperature conditions and observed monomer and dimer product ion peaks at 1.42 and 1.06 cm^{2}V^{-1}s^{-1}, respectively.[18] When TEPO was introduced into the AIMI drift tube, an ammoniated monomer ion of TEPO [(TEPO)NH$_4^+$, *m/z* 200] and an ammonium-bound dimer ion of TEPO [(TEPO)$_2$NH$_4^+$, *m/z* 382] were observed. The protonated monomer ion of TEPO [(TEPO)H$^+$, *m/z* 183] was also present in the mass spectrum, but it was only a fragment of (TEPO)NH$_4^+$ in the TOFMS interface and not freely formed in the drift tube. The proton-bound dimer ion of TEPO [(TEPO)$_2$H$^+$, *m/z* 365] was not present in the ion mass-mobility spectrum. The influence of drift gas water content and temperature are shown for the monomer and dimer ion K_0 values in Figure 3a,b.

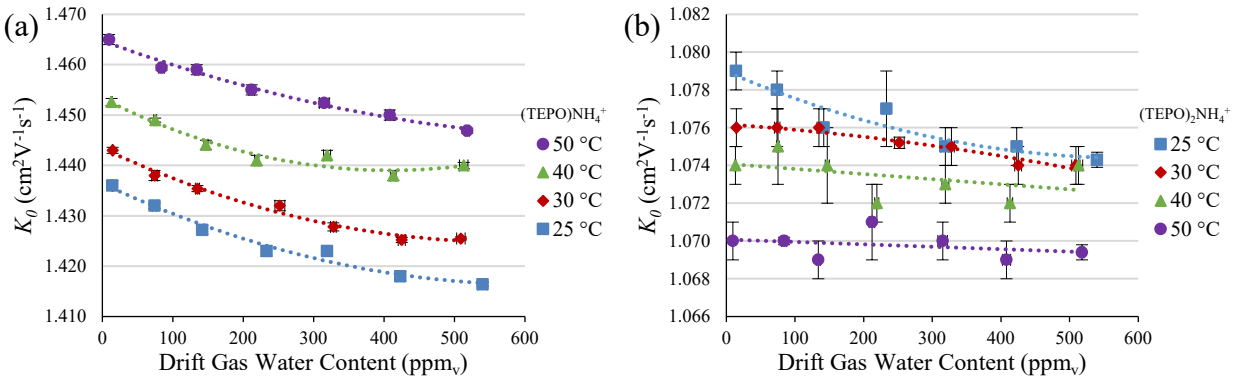

Figure 3. Effect of drift gas water content on the K_0 values of (a) $(TEPO)NH_4^+$ and (b) $(TEPO)_2NH_4^+$ at 25.0 ± 0.1 (■), 30.0 ± 0.1 (◆), 40.2 ± 0.1 (▲), and 50.0 ± 0.1 (●) °C.

The K_0 value of $(TEPO)NH_4^+$ at 25 °C and under dry drift gas conditions was 1.436 ± 0.001 $cm^2V^{-1}s^{-1}$, which was 1.1% higher than the value measured by Satoh et al.[18] Analysis of $(TEPO)NH_4^+$ produced a range of K_0 values between 1.465 ± 0.001 and 1.4164 ± 0.0004 $cm^2V^{-1}s^{-1}$ for the conditions studied. The K_0 value of $(TEPO)NH_4^+$ was also sensitive to changes in drift gas water content and decreased in a second-degree polynomial fashion with increasing water vapor concentration. The K_0 value of $(TEPO)NH_4^+$ decreased as a function of water vapor concentration by 1.4, 1.2, 0.9, and 1.2% at 25, 30, 40, and 50 °C, respectively. The K_0 value of $(TEPO)NH_4^+$ was less sensitive to changes in the drift gas water content than was the ammoniated monomer ion of DMMP $[(DMMP)NH_4^+]$, which decreased between 3 and 4% under approximately the same conditions.[5]

The K_0 value of $(TEPO)_2NH_4^+$ at 25 °C and under dry drift gas conditions was 1.0785 ± 0.0008 $cm^2V^{-1}s^{-1}$, which was 1.7% higher than the value measured by Satoh et al.[18] Compared with other dimer species, analysis of $(TEPO)_2NH_4^+$ produced a wide range of K_0 values between 1.069 ± 0.001 and 1.0785 ± 0.0008 $cm^2V^{-1}s^{-1}$ and exhibited unique trends. An increase in temperature caused a decrease in its K_0 value at all drift gas water content conditions. The 50 °C trend line had a linear R^2 value of 0.11 and an average value of 1.0698 ± 0.0007 $cm^2V^{-1}s^{-1}$, with a range from 1.069 ± 0.001 to 1.071 ± 0.002 $cm^2V^{-1}s^{-1}$. As the drift gas temperature decreased, the K_0 value of $(TEPO)_2NH_4^+$ became more sensitive to drift gas water content. The 40 °C trend line shown in Figure 3b was also linear, whereas the 25 and 30 °C trend lines were second-degree polynomials. The K_0 values of $(TEPO)_2NH_4^+$ decreased as a function of water vapor concentration by 0.4 and 0.2% at 25 and 30 °C, respectively, which was similar to the degree of change seen in the K_0 value of the ammonium-bound dimer ion of DMMP $[(DMMP)_2NH_4^+]$.[5] This behavior may be due to a temperature-dependent conformation change in $(TEPO)_2NH_4^+$ that was similar to what was previously proposed for the behavior exhibited by $(DMMP)_2NH_4^+$.[5] It is proposed that as the drift gas temperature was increased, the conformation of the ion may change from two TEPO molecules attached to two different hydrogens of NH_4^+ to an NH_3 molecule attached to a hydrogen of $(TEPO)_2H^+$. It appeared that such a temperature-dependent conformational change also caused a change in the degree to which the K_0 value of $(TEPO)_2NH_4^+$ was sensitive to changes in drift gas water content. Although $(TEPO)NH_4^+$ would be an appropriate environmental standard due to its response to drift gas water content and

temperature, the complex influence of temperature and drift gas water content on the K_0 value of $(TEPO)_2NH_4^+$ indicates that it would not be a suitable instrumental standard.

3.4 DPM

DPM was previously proposed as an ion mobility reference standard for its relatively high vapor pressure (0.28 mmHg at 20 °C) and for its ability to produce positive ion monomer and dimer species.[3] However, DPM contains an inseparable mixture of isomers when manufactured. This may cause a wider spread in the arrival time distribution and result in different K_0 values based on each isomer's slightly different collision cross section. Like TEPO, there is not an agreed upon K_0 value for the ions that are produced with DPM, and varying dopant conditions for DPM can be found in published studies.[19–21] Hill and Thomas reported K_0 values for DPM at 40 °C, with 75 mg/m^3 (113 ppm$_v$) drift gas water content, and under ammoniated conditions for nickel-63 and pulsed corona discharge ionization sources. The product ions observed in their study were an ammoniated monomer ion of DPM [$(DPM)NH_4^+$, *m/z* 166] and ammonium-bound dimer ion of DPM [$(DPM)_2NH_4^+$, *m/z* 314] for both ionization sources. The K_0 values for the monomer and dimer ions were 1.47 and 1.17 cm^{2}V^{-1}s^{-1}, respectively.[21] The same DPM product ions were seen in this study upon introduction into the AIMI drift tube, and protonated species were not present in the mass spectrum. The effect of drift gas water content and temperature on the K_0 values of the $(DPM)NH_4^+$ and $(DPM)_2NH_4^+$ are shown in Figure 4a,b.

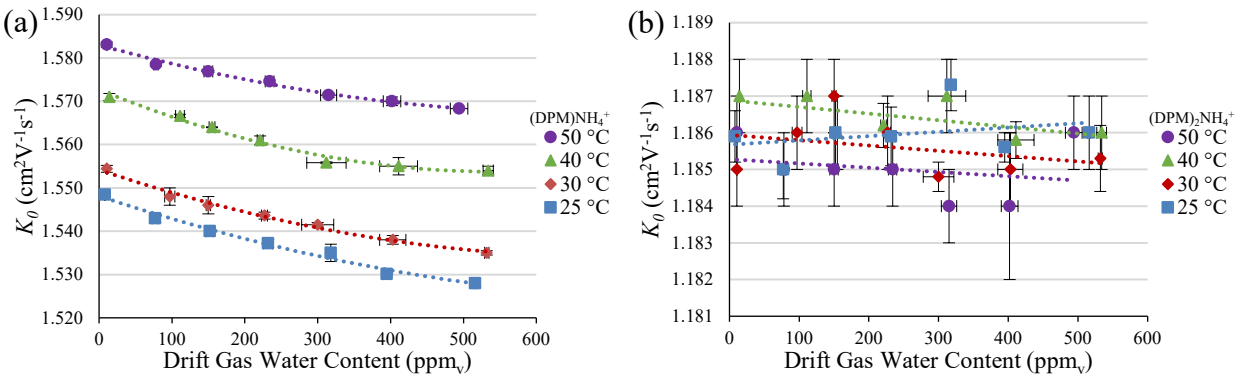

Figure 4. Effect of drift gas water content on the K_0 values of (a) $(DPM)NH_4^+$ and (b) $(DPM)_2NH_4^+$ at 25.06 ± 0.03 (■), 29.99 ± 0.03 (◆), 39.99 ± 0.03 (▲), and 49.99 ± 0.03 (●) °C.

$(DPM)NH_4^+$ produced a range of K_0 values between 1.528 ± 0.001 and 1.583 ± 0.001 cm^{2}V^{-1}s^{-1}. Between the highest and lowest drift gas water contents, the K_0 value of $(DPM)NH_4^+$ decreased in a second-degree polynomial fashion by 1.3, 1.2, 1.1, and 0.9% at 25, 30, 40, and 50 °C, respectively. When the 40 °C trend line in Figure 4a was used to calculate the K_0 value of $(DPM)NH_4^+$ at 113 ppm$_v$, the value was 1.566 cm^{2}V^{-1}s^{-1}, which was 6.5% higher than the value reported by Hill and Thomas. The average K_0 value of $(DPM)_2NH_4^+$ in Figure 4b was 1.1857 ± 0.0009 cm^{2}V^{-1}s^{-1}, which was 1.3% higher than the value reported by Hill and Thomas.[21] The lowest and highest K_0 values for $(DPM)_2NH_4^+$ in Figure 4b were 1.184 ± 0.002 and 1.187 ± 0.001 cm^{2}V^{-1}s^{-1}, respectively. The linear R^2 values of each trend line in Figure 4b

were also low at 0.08, 0.17, 0.30, and 0.06 for 25, 30, 40, and 50 °C, respectively, and they indicated no correlation between K_0 value and drift gas water content at each evaluated temperature. This indicated that the ammoniated DPM dimer ion was an appropriate instrumental standard and was similar to D*t*BP, and the ammoniated DPM monomer ion was an appropriate environmental standard.

The large percentage difference between the $(DPM)NH_4^+$ K_0 value reported by Hill and Thomas and our own value may be due to differences in ammonia dopant concentration or accuracy in the K_0 value calculation. Hill and Thomas reported an ammonia dopant concentration of 1.3 mg/m^3 (1.9 ppm_v),[21] whereas our concentration was 20 ppm_v. Such a low concentration may not have been enough to minimize the clustering effects of water, or there may have been a larger mixture of water and ammonia clusters around their ions. Alternatively, Hill and Thomas reported a drift gas temperature of 40 °C used for calculations but did not indicate whether this value was directly measured, nor did they mention temperature gradients across the ion drift region. If neither was accounted for, the true drift gas temperature was likely less than 40 °C, which would have lowered the calculated K_0 value of the monomer on the basis of the measured drift times. Due to the insensitivity of the $(DPM)_2NH_4^+$ K_0 value to changes in both temperature and drift gas water content, this effect would not have been seen as much for the dimer ion and would account for the lower percent difference between their values and ours.

3.5 MES

MES is a commonly used ion mobility reference standard that has a relatively high vapor pressure (0.1 Torr at 20 °C) and has shown activity in both ionization modes. However, it is only active in the positive ion detection mode under extremely dry conditions, which may be hard to achieve outside of the laboratory.[3] Few studies offer an ab initio calculation of MES K_0 values, perhaps because of its frequent use as an internal calibrant and because the traditional value of 1.474 $cm^2V^{-1}s^{-1}$ is used for negative ion detection mode calibration.[3] Patchett et al. reported a negative ion detection mode value of 1.62 $cm^2V^{-1}s^{-1}$ using an Ionscan 350 system (Smiths Detection) at 92 °C with a hexachloroethane dopant in dry air and with an nickel-63 ionization source. However, this MES K_0 value was not mass-identified or specified as having been calculated ab initio.[22] Roscioli et al. used a laboratory IMS–TOFMS operated at 160 °C and 304 V/cm in the negative ion detection mode, with a 2.5 L/min flow of N_2 drift gas, and a desorption electrospray ionization source. They measured a K_0 value of 1.49 $cm^2V^{-1}s^{-1}$ for the proton-abstracted ion of MES [$(MES–H)^–$; *m/z* 151].[23] Davis et al. reported a value of 1.57 $cm^2V^{-1}s^{-1}$ on an instrument using voltage-sweep programming. However, neither the water vapor content nor the temperature of the compressed air drift gas were specified, and the ion was not mass-identified.[24] Ross and Bell reported a K_0 value of 1.56 $cm^2V^{-1}s^{-1}$ for the oxygen adduct ion of MES [$(MES•O_2)^–$; *m/z* 184] at 200 V/cm, with dry air (10 ppm_v H_2O) as the drift gas and with both reverse-flow corona and nickel-63 ionization sources. The authors did not specify the temperature of the drift gas.[25] Crawford et al. offered the most extensive analysis of MES with values between 1.340 ± 0.007 and 1.470 ± 0.005 $cm^2V^{-1}s^{-1}$ for $(MES–H)^–$ using compressed air as the drift gas and nickel-63 ionization. The range of values were reported at drift gas water contents of 4 and 2100 mg/m^3 at 34.8 ± 0.4 and 49.10 ± 0.5 °C, respectively. At 96.9 ± 0.6 and 145.3 ± 0.4 °C, the primary product ion shifted to the carbon

dioxide adduct of MES [$(MES•CO_2)^-$; *m/z* 196] and produced K_0 values between 1.580 ± 0.007 and 1.650 ± 0.007 $cm^2V^{-1}s^{-1}$ for the same drift gas water content conditions.[9]

When MES was introduced in the AIMI drift tube at 25 °C and under dry conditions, $(MES•O_2)^-$ was produced. An increase in the drift gas water content caused the product ion to shift to both $(MES–H)^-$ and an *m/z* 166 ion, which was thought to be the water-abstracted ion of MES [$(MES•O_2–H_2O)^-$]. Each of these two product ions are distinct with their own, but similar, K_0 values. For example, at 25 °C and 151 ppm_v drift gas water content, the K_0 values of $(MES–H)^-$ and $(MES•O_2–H_2O)^-$ were 1.556 ± 0.002 and 1.5421 ± 0.0008 $cm^2V^{-1}s^{-1}$, respectively. Because most fielded IMS systems do not possess the resolving power to separate such closely spaced ion mobility peaks, an internal Faraday plate that was positioned before the TOFMS inlet was used to analyze the two peaks. The drift length was calculated to be 16.433 cm on the basis of the average K_0 value of $(DtBP)H^+$ reported herein. As was expected, a single unresolved peak was observed, and its K_0 values fell between the two mass-identified ion mobility peaks, as shown in Figure 5.

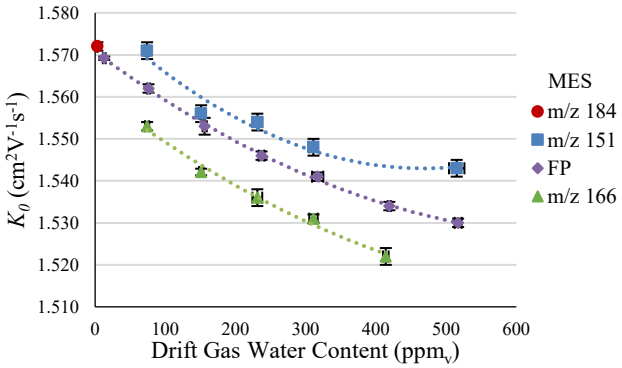

Figure 5. Effect of drift gas water content on the product ions and K_0 values of MES at 25.07 ± 0.04 °C for $(MES•O_2)^-$ (*m/z* 184, ●); $(MES–H)^-$ (*m/z* 151, ■); and $(MES•O_2–H_2O)^-$ (*m/z* 166, ▲). A single, unresolved ion mobility peak was observed when measured with an internal Faraday plate (FP; ◆).

In addition to the creation of a complicated product ion chemistry, the introduction of water vapor into the drift gas caused the product ion peak height to significantly decrease. Under dry drift gas conditions, the MES product ion peak easily formed and the reactant ion peak could be eliminated if the concentration was too high. Figure 6 shows a spectrum at 2.82 ± 0.01 ppm_v drift gas water content (Figure 6, black trace) with the product ion peak at 48% of the height of the reactant ion peak. Upon introduction of water into the drift gas at 74 ± 2 ppm_v (Figure 6, red trace), the product ion peak height was reduced to 6% of the reactant ion peak height. The product ion peak height could not be increased far beyond this level without increasing the bridging between the reactant and product ion peaks. Increasing the drift gas water content caused a greater degree of fragmentation and bridging between the product ion and reactant ion peaks. Because of these spectrum issues, which arose with changes in environmental conditions, MES was not considered to be a suitable standard for accurate IMS calibration.

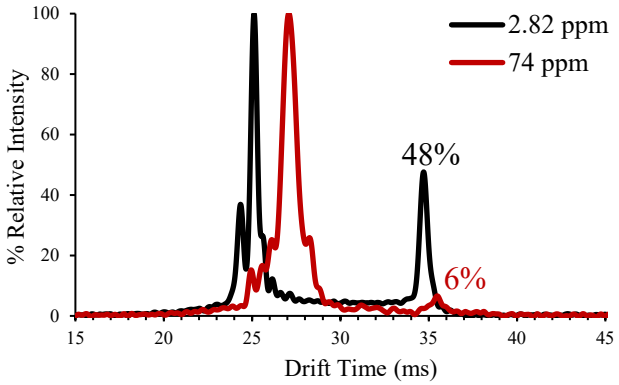

Figure 6. Spectra of MES at 25.07 ± 0.04 °C, showing the product ion peak height decreasing from 48% of the reactant ion peak height at 2.82 ± 0.01 ppm_v H_2O drift gas water content (black trace) to 6% at 74 ± 2 ppm_v H_2O drift gas water content (red trace).

3.6 K_0 Values of Chemical Standards Studied

The accurate K_0 values of D*t*BP, TEPO, DPM, and MES (used to create Figures 2–5) are shown in Tables 1–4. K_0 values of PDO are not listed because no viable ion mobility spectra of PDO could be collected under ammoniated conditions. Each data point is an average of three measurements with the precision represented by error bars in Figures 2–5; error bars are hidden by the marker when not visible.

Table 1. K_0 Values of (D*t*BP)H^+ at 280.1 V/cm as a Function of Drift Gas Water Content at Four Drift Gas Temperatures

Average Drift Gas Temperature (°C)	**Average Drift Gas Water Content (ppm_v H_2O)**	**K_0 Value (precision, accuracy) ($cm^2V^{-1}s^{-1}$) (D*t*BP)H^+ *m/z* 192**
25.0 ± 0.1	10.7 ± 0.3	1.479 (± 0.001, ± 0.001)
	75 ± 3	1.478 (± 0.002, ± 0.002)
	157 ± 3	1.4763 (± 0.0005, ± 0.001)
	224 ± 4	1.4776 (± 0.0009, ± 0.001)
	350 ± 19	1.4785 (± 0.0005, ± 0.001)
	413 ± 10	1.4771 (± 0.0005, ± 0.001)
	515 ± 7	1.475 (± 0.001, ± 0.001)
30.0 ± 0.1	11.1 ± 0.1	1.478 (± 0.001, ± 0.001)
	74.5 ± 0.3	1.478 (± 0.001, ± 0.001)
	144 ± 4	1.476 (± 0.001, ± 0.001)
	241 ± 2	1.478 (± 0.001, ± 0.001)
	344 ± 4	1.479 (± 0.001, ± 0.001)
	406 ± 4	1.4783 (± 0.0003, ± 0.001)
	509 ± 6	1.4771 (± 0.0009, ± 0.001)
40.2 ± 0.1	13.9 ± 0.1	1.4765 (± 0.0007, ± 0.001)
	82 ± 2	1.4758 (± 0.0007, ± 0.001)
	153 ± 2	1.4758 (± 0.0004, ± 0.001)
	228 ± 3	1.476 (± 0.001, ± 0.001)
	364 ± 14	1.475 (± 0.002, ± 0.002)
	418 ± 4	1.474 (± 0.001, ± 0.001)
	532 ± 2	1.476 (± 0.002, ± 0.002)
50.0 ± 0.1	10.3 ± 0.6	1.476 (± 0.001, ± 0.001)
	82.3 ± 0.2	1.477 (± 0.001, ± 0.001)
	132 ± 2	1.4769 (± 0.0009, ± 0.001)
	239 ± 2	1.4753 (± 0.0007, ± 0.001)
	312 ± 9	1.4764 (± 0.0004, ± 0.001)
	416 ± 4	1.4760 (± 0.0005, ± 0.001)
	516 ± 3	1.477 (± 0.001, ± 0.001)

Note: The precision followed by the accuracy of each data point are reported in parentheses.

Table 2. K_0 Values of $(TEPO)NH_4^+$ and $(TEPO)_2NH_4^+$ at 280.1 V/cm as a Function of Drift Gas Water Content at Four Drift Gas Temperatures

Average Drift Gas Temperature (°C)	**Average Drift Gas Water Content (ppm_v H_2O)**	**K_0 Value (precision, accuracy) ($cm^2V^{-1}s^{-1}$)**	
		$TEPONH_4^+$ *m/z* 200	**$(TEPO)_2NH_4^+$ *m/z* 382**
25.0 ± 0.1	14.1 ± 0.6	1.436 (± 0.001, ± 0.001)	1.0785 (± 0.0008, ± 0.001)
	74 ± 3	1.4320 (± 0.0006, ± 0.001)	1.0779 (± 0.0005, ± 0.001)
	142 ± 4	1.4272 (± 0.0009, ± 0.001)	1.076 (± 0.001, ± 0.001)
	233 ± 5	1.423 (± 0.001, ± 0.001)	1.077 (± 0.002, ± 0.002)
	319 ± 7	1.423 (± 0.001, ± 0.001)	1.075 (± 0.001, ± 0.001)
	423 ± 5	1.418 (± 0.001, ± 0.001)	1.075 (± 0.001, ± 0.001)
	540 ± 7	1.4164 (± 0.0004, ± 0.001)	1.0743 (± 0.0004, ± 0.001)
30.0 ± 0.1	15.5 ± 0.5	1.4430 (± 0.0006, ± 0.001)	1.076 (± 0.001, ± 0.001)
	74 ± 4	1.438 (± 0.001, ± 0.001)	1.076 (± 0.001, ± 0.001)
	135 ± 3	1.4354 (± 0.0006, ± 0.001)	1.076 (± 0.001, ± 0.001)
	252 ± 7	1.432 (± 0.001, ± 0.001)	1.0752 (± 0.0003, ± 0.001)
	328 ± 4	1.4278 (± 0.0008, ± 0.001)	1.075 (± 0.001, ± 0.001)
	425 ± 5	1.4252 (± 0.0005, ± 0.001)	1.074 (± 0.001, ± 0.001)
	509 ± 6	1.4255 (± 0.0003, ± 0.001)	1.074 (± 0.001, ± 0.001)
40.2 ± 0.1	13.1 ± 0.8	1.4526 (± 0.0007, ± 0.001)	1.0745 (± 0.0007, ± 0.001)
	75 ± 2	1.4490 (± 0.0004, ± 0.001)	1.075 (± 0.002, ± 0.002)
	147 ± 3	1.4441 (± 0.0009, ± 0.001)	1.074 (± 0.002, ± 0.002)
	219 ± 3	1.441 (± 0.001, ± 0.001)	1.072 (± 0.001, ± 0.001)
	319 ± 5	1.442 (± 0.001, ± 0.001)	1.073 (± 0.001, ± 0.001)
	413 ± 4	1.438 (± 0.001, ± 0.001)	1.0724 (± 0.0008, ± 0.001)
	513 ± 6	1.4400 (± 0.0006, ± 0.001)	1.0736 (± 0.0007, ± 0.001)
50.0 ± 0.1	9.5 ± 0.1	1.465 (± 0.001, ± 0.001)	1.070 (± 0.001, ± 0.001)
	84 ± 4	1.4594 (± 0.0005, ± 0.001)	1.0700 (± 0.0002, ± 0.001)
	134 ± 3	1.459 (± 0.001, ± 0.001)	1.069 (± 0.001, ± 0.001)
	212 ± 4	1.455 (± 0.001, ± 0.001)	1.071 (± 0.002, ± 0.001)
	315 ± 7	1.4524 (± 0.0008, ± 0.001)	1.0700 (± 0.0008, ± 0.001)
	408 ± 6	1.450 (± 0.001, ± 0.001)	1.069 (± 0.001, ± 0.001)
	518 ± 3	1.4469 (± 0.0005, ± 0.001)	1.0694 (± 0.0004, ± 0.001)

Note: The precision followed by the accuracy of each data point are reported in parentheses.

Table 3. K_0 Values of $(DPM)NH_4^+$ and $(DPM)_2NH_4^+$ at 280.1 V/cm as a Function of Drift Gas Water Content at Four Drift Gas Temperatures

Average Drift Gas Temperature (°C)	**Average Drift Gas Water Content (ppm_v H_2O)**	**K_0 Value (precision, accuracy) ($cm^2V^{-1}s^{-1}$)**	
		$DPMH_4^+$ *m/z* 166	**$(DPM)_2NH_4^+$ *m/z* 314**
25.06 ± 0.03	7.95 ± 0.01	1.5484 (± 0.0004, ± 0.002)	1.1859 (± 0.0007, ± 0.001)
	77 ± 4	1.543 (± 0.001, ± 0.002)	1.1850 (± 0.0008, ± 0.001)
	152 ± 5	1.540 (± 0.001, ± 0.002)	1.186 (± 0.001, ± 0.001)
	232 ± 6	1.5372 (± 0.0009, ± 0.002)	1.1859 (± 0.0008, ± 0.001)
	318 ± 6	1.535 (± 0.002, ± 0.002)	1.1873 (± 0.0007, ± 0.001)
	395 ± 5	1.5301 (± 0.0002, ± 0.002)	1.1856 (± 0.0004, ± 0.001)
	516 ± 2	1.528 (± 0.001, ± 0.002)	1.186 (± 0.001, ± 0.001)
29.99 ± 0.03	10.7 ± 0.1	1.5544 (± 0.0008, ± 0.002)	1.185 (± 0.001, ± 0.001)
	97 ± 7	1.548 (± 0.002, ± 0.002)	1.186 (± 0.001, ± 0.001)
	150 ± 3	1.546 (± 0.002, ± 0.002)	1.187 (± 0.001, ± 0.001)
	227 ± 4	1.5436 (± 0.0008, ± 0.002)	1.186 (± 0.001, ± 0.001)
	300 ± 22	1.5415 (± 0.0005, ± 0.002)	1.1848 (± 0.0004, ± 0.001)
	403 ± 18	1.538 (± 0.001, ± 0.002)	1.185 (± 0.001, ± 0.001)
	532 ± 3	1.5350 (± 0.0005, ± 0.002)	1.1853 (± 0.0009, ± 0.001)
39.99 ± 0.03	14.1 ± 0.1	1.5710 (± 0.0008, ± 0.002)	1.187 (± 0.001, ± 0.001)
	111 ± 6	1.5666 (± 0.0004, ± 0.002)	1.187 (± 0.001, ± 0.001)
	155 ± 4	1.5640 (± 0.001, ± 0.002)	1.186 (± 0.001, ± 0.001)
	221 ± 4	1.561 (± 0.001, ± 0.002)	1.1862 (± 0.0006, ± 0.001)
	312 ± 27	1.5558 (± 0.0002, ± 0.002)	1.187 (± 0.001, ± 0.001)
	411 ± 26	1.555 (± 0.002, ± 0.002)	1.1858 (± 0.0005, ± 0.001)
	534 ± 7	1.554 (± 0.001, ± 0.002)	1.186 (± 0.001, ± 0.001)
49.99 ± 0.03	10.6 ± 0.3	1.5831 (± 0.0006, ± 0.002)	1.186 (± 0.001, ± 0.001)
	78 ± 3	1.5785 (± 0.0004, ± 0.002)	1.185 (± 0.001, ± 0.001)
	150 ± 6	1.5769 (± 0.0002, ± 0.002)	1.185 (± 0.001, ± 0.001)
	234 ± 6	1.5746 (± 0.0003, ± 0.002)	1.185 (± 0.001, ± 0.001)
	315 ± 11	1.5714 (± 0.0005, ± 0.002)	1.184 (± 0.001, ± 0.001)
	402 ± 12	1.570 (± 0.001, ± 0.002)	1.184 (± 0.002, ± 0.002)
	494 ± 12	1.5683 (± 0.0003, ± 0.002)	1.186 (± 0.001, ± 0.001)

Note: The precision followed by the accuracy of each data point are reported in parentheses.

Table 4. K_0 values of $(MES•O_2)^-$, $(MES–H)^-$, and a Possible Conformational Fragment $(MES•O_2–H_2O)^-$ Detected at 280.2 V/cm with the IMS–TOFMS, and the K_0 Values of the MES Monomer Product Ion Peak Detected at 278.8 V/cm with the IMS Faraday Plate.

Detection Method	**Ion Identity**	**Average Drift Gas Water Content (ppm_v H_2O)**	**K_0 Value (precision, accuracy) ($cm^2V^{-1}s^{-1}$)**
IMS–TOFMS	$(MES•O_2)^-$ *m/z* 184	3.2 ± 0.3	1.572 (± 0.001, ± 0.002)
IMS–TOFMS	$(MES–H)^-$ *m/z* 151	74 ± 3	1.571 (± 0.002, ± 0.002)
		151 ± 3	1.556 (± 0.002, ± 0.002)
		231 ± 7	1.554 (± 0.002, ± 0.002)
		311 ± 6	1.548 (± 0.002, ± 0.002)
		515 ± 11	1.543 (± 0.002, ± 0.002)
IMS–TOFMS	$(MES•O_2–H_2O)^-$ *m/z* 166	74 ± 3	1.553 (± 0.001, ± 0.002)
		151 ± 3	1.5421 (± 0.0008, ± 0.002)
		231 ± 7	1.536 (± 0.002, ± 0.002)
		311 ± 6	1.531 (± 0.001, ± 0.002)
		414 ± 4	1.522 (± 0.002, ± 0.002)
Faraday plate	Monomer product ion peak	13 ± 2	1.5692 (± 0.0004, ± 0.002)
		76 ± 2	1.562 (± 0.001, ± 0.002)
		156 ± 3	1.553 (± 0.002, ± 0.002)
		237 ± 4	1.546 (± 0.001, ± 0.002)
		317 ± 8	1.541 (± 0.001, ± 0.002)
		419 ± 2	1.534 (± 0.001, ± 0.002)
		517 ± 5	1.530 (± 0.001, ± 0.002)

Note: K_0 values are reported at 25.07 ± 0.04 °C as a function of drift gas water content. The precision followed by the accuracy of each data point are reported in parentheses.

4. CONCLUSIONS

Five potential IMS calibrant compounds, four for the positive ion detection mode and one for the negative ion detection mode, were accurately evaluated as a function of drift gas temperature and water content. PDO was not recommended for systems that use an ammonia dopant because of the instability and fragmentation of ammoniated dimer species. Similarly, MES was not recommended for use in calibration due to its instability and changing ion chemistry with even a small increase in drift gas humidity. Although only a 25 °C drift gas temperature for MES was studied herein, an increase in the drift gas temperature may continue to complicate these ion chemistry and signal issues, as was seen in previous studies. $(TEPO)_2NH_4^+$ also exhibited complicated trends in its K_0 value as a function of drift gas temperature and humidity, which eliminated it as a suitable calibrant as well. DPM was found to be the best of the calibrants observed in this study. It produced both monomer and dimer species, and the monomer K_0 value was sensitive to changes in drift gas water content and temperature, whereas the dimer K_0 value remained relatively constant at 1.1857 ± 0.0009 $cm^2V^{-1}s^{-1}$ under the conditions studied herein. If a negative ion detection mode calibrant does not produce monomer and dimer species, the monomer and dimer K_0 values of DPM could be used to empirically measure the drift gas

water content as part of the accurate calibration procedure. D*t*BP is an acceptable positive ion mobility calibrant with an average K_0 value of 1.477 ± 0.001 $cm^2V^{-1}s^{-1}$ across the range of conditions studied herein. The K_0 value of (D*t*BP)H^+ is insensitive to changes in temperature and drift gas water content, but does not produce a dimer ion. If it is to be used for calibration in the positive ion detection mode, the negative ion detection mode calibrant would therefore need to be one that produces monomer and dimer species for drift gas water content measurement. A suitable ion mobility calibrant for the negative ion detection mode has yet to be accurately analyzed, but IsoF could be a candidate because it is active in the negative ion detection mode and produces both monomer and dimer species.

Blank

LITERATURE CITED

1. Eiceman, G.A.; Stone, J.A. Ion Mobility Spectrometers in National Defense. *Anal. Chem.* **2004,** *76* (21), 390A–397A.

2. Eiceman, G.A.; Karpas, Z.; Hill, H.H., Jr. *Ion Mobility Spectrometry*, 3rd ed.; CRC Press: Boca Raton, FL, 2013.

3. Hauck, B.C.; Harden, C.S.; McHugh, V.M. Current Status and Need for Standards in Ion Mobility Spectrometry. *Int. J. Ion Mobil. Spectrom.* **2018,** *21* (4), 105–123.

4. Hauck, B.C.; Siems, W.F.; Harden, C.S.; McHugh, V.M.; Hill, H.H., Jr. Construction and Evaluation of a Hermetically Sealed Accurate Ion Mobility Instrument. *Int. J. Ion Mobil. Spec.* **2017,** *20* (3–4), 57–66.

5. Hauck, B.C.; Siems, W.F.; Harden, C.S.; McHugh, V.M.; Hill, H.H., Jr. High Accuracy Ion Mobility Spectrometry for Instrument Calibration. *Anal. Chem.* **2018,** *90* (7), 4578–4584.

6. Hauck, B.C.; Siems, W.F.; Harden, C.S.; McHugh, V.M.; Hill, H.H., Jr. Determination of E/N Influence on K_0 Values within the Low Field Region of Ion Mobility Spectrometry. *J. Phys. Chem. A* **2017,** *121* (11), 2274–2281.

7. Hauck, B.C.; Siems, W.F.; Harden, C.S.; McHugh, V.M.; Hill, H.H., Jr. E/N Effects on K_0 Values Revealed by High Precision Measurements under Low Field Conditions. *Rev. Sci. Instrum.* **2016,** *87* (7), 075104.

8. Hauck, B.C.; Davis, E.J.; Clark, A.E.; Siems, W.F.; Harden, C.S.; McHugh, V.M.; Hill, H.H., Jr. Determining the Water Content of a Drift Gas Using Reduced Ion Mobility Measurements. *Int. J. Mass Spectrom.* **2014,** *368,* 37–44.

9. Crawford, C.L.; Hauck, B.C.; Tufariello, J.A.; Harden, C.S.; McHugh, V.; Siems, W.F.; Hill, H.H., Jr. Accurate and Reproducible Ion Mobility Measurements for Chemical Standard Evaluation. *Talanta* **2012,** *101,* 161–170.

10. Fernández-Maestre, R.; Harden, C.S.; Ewing, R.G.; Crawford, C.L.; Hill, H.H., Jr. Chemical Standards in Ion Mobility Spectrometry. *Analyst* **2010,** *135* (6), 1433–1442.

11. McIntyre, H.; Thathapudi, N.; Arnold, P. Chemical Calibration Process, System and Device. U.S. Patent 9,945,813; 17 April 2018.

12. Rajapakse, M.Y.; Fowler, P.E.; Eiceman, G.A.; Stone, J.A. Dissociation Enthalpies of Chloride Adducts of Nitrate and Nitrite Explosives Determined by Ion Mobility Spectrometry. *J. Phys. Chem. A* **2016,** *120* (5), 690–698.

13. Eiceman, G.A.; Nazarov, E.G.; Stone, J.A. Chemical Standards in Ion Mobility Spectrometry. *Anal. Chim. Acta* **2003,** *493* (2), 185–194.

14. Viitanen, A.-K.; Mauriala, T.; Mattila, T.; Adamov, A.; Pederson, C.S.; Mäkelä, J.M.; Marjamäki, M.; Sysoev, A.; Keskinen, J.; Kotiaho, T. Adjusting Mobility Scales of Ion Mobility Spectrometers Using 2,6-D*t*BP as a Reference Compound. *Talanta* **2008,** *76* (5), 1218–1223.

15. Valadbeigi, Y.; Ilbeigi, V.; Michalczuk, B.; Sabo, M.; Matejcik, S. Study of Atmospheric Pressure Chemical Ionization Mechanism in Corona Discharge Ion Source with and without NH_3 Dopant by Ion Mobility Spectrometry Combined with Mass Spectrometry: A Theoretical and Experimental Study. *J. Phys. Chem. A* **2019,** *123* (1), 313–322.

16. Cao, L.B.; Harrington, P.D.; Liu, C. Two-Dimensional Nonlinear Wavelet Compression of Ion Mobility Spectra of Chemical Warfare Agent Simulants. *Anal. Chem.* **2004,** *76* (10), 2859–2868.

17. Eiceman, G.A.; Wang, Y.F.; Garcia-Gonzalez, L.; Harden, C.S.; Shoff, D.B. Enhanced Selectivity in Ion Mobility Spectrometry Analysis of Complex Mixtures by Alternate Reagent Gas Chemistry. *Anal. Chim. Acta* **1995,** *306* (1), 21–33.

18. Satoh, T.; Kishi, S.; Nagashima, H.; Tachikawa, M.; Kanamori-Kataoka, M.; Nakagawa, T.; Kitagawa, N.; Tokita, K.; Yamamoto, S.; Seto, Y. Ion Mobility Spectrometric Analyis of Vaporous Chemical Warfare Agents by the Instrument with Corona Discharge Ionization Ammonia Dopant Ambient Temperature Operation. *Anal. Chim. Acta* **2015,** *865,* 39–52.

19. Kaur-Atwal, G.; O'Connor, G.; Aksenov, A.A.; Bocos-Bintintan, V.; Thomas, C.L.P.; Creaser, C.S. Chemical Standards for Ion Mobility Spectrometry: A Review. *Int. J. Ion Mobil. Spectrom.* **2009,** *12* (1), 1–14.

20. Preston, J.M.; Rajadhyax, L. Effect of Ion/Molecule Reactions on Ion Mobilities. *Anal. Chem.* **1988,** *60* (1), 31–34.

21. Hill, C.A.; Thomas, C.L.P. Programmable Gate Delayed Ion Mobility Spectrometry-Mass Spectrometry: A Study with Low Concentrations of Dipropylene-glycol-monomethyl-ether in Air. *Analyst* **2005,** *130* (8), 1155–1161.

22. Patchett, M.L.; Minoshima, Y.; Harrington, P.B. Detection of Gamma-Hydroxybutyrate and Gamma-Butyrolactone by Ion Mobility Spectrometry. *Spectroscopy* **2002,** *17* (11), 16–24.

23. Roscioli, K.M.; Tufariello, J.A.; Zhang, X.; Li, S.X.; Goetz, G.H.; Cheng, G.L.; Siems, W.F.; Hill, H.H., Jr. Desorption Electrospray Ionization (DESI) with Atmospheric Pressure Ion Mobility Spectrometry for Drug Detection. *Analyst* **2014,** *139* (7), 1740–1750.

24. Davis, E.J.; Williams, M.D.; Siems, W.F.; Hill, H.H., Jr. Voltage Sweep Ion Mobility Spectrometry. *Anal. Chem.* **2011,** *83* (4), 1260–1267.

25. Ross, S.K.; Bell, A.J. Reverse Flow Continuous Corona Discharge Ionisation Applied to Ion Mobility Spectrometry. *Int. J. Mass Spectrom.* **2002,** *218* (2), L1–L6.

Blank

ACRONYMS AND ABBREVIATIONS

AIMI	accurate ion mobility instrument
BN	Bradbury–Nielson
DMMP	dimethyl methylphosphonate
$(DMMP)NH_4^+$	ammoniated monomer ion of DMMP
$(DMMP)_2NH_4^+$	ammonium-bound dimer ion of DMMP
DPM	di(propylene glycol) methyl ether
$(DPM)NH_4^+$	ammoniated monomer ion of DPM
$(DPM)_2NH_4^+$	ammonium-bound dimer ion of DPM
D*t*BP	2,6-di-*tert*-butylpyridine
$(DtBP)H^+$	protonated monomer ion of D*t*BP
$(DtBP)NH_4^+$	ammoniated monomer ion of D*t*BP
FP	Faraday plate
$H(H_2O)_n^+$	water reactant ions
$H(NH3)_n^+$	ammonia reactant ions
HPLC	high-performance liquid chromatography
IMS	ion mobility spectrometry
IsoF	isoflurane
K_0	reduced ion mobility
$K_{0\ cal}$	reduced ion mobility of calibrant compound calculated by an uncalibrated instrument
$K_{0\ det}$	calibrated reduced ion mobility value of a chemical of interest to be used for identification and alarm detection purposes
$K_{0\ obs}$	initially calculated reduced ion mobility value of a chemical of interest or unknown peak
$K_{0\ std}$	reduced ion mobility value of a calibrant standard
L	length
LCD	lightweight chemical detector
MES	methyl salicylate
$(MES•CO_2)^-$	carbon dioxide adduct ion of MES
$(MES–H)^-$	proton-abstracted ion of MES
$(MES•O_2)^-$	oxygen adduct ion of MES
$(MES•O_2–H_2O)^-$	water-abstracted oxygen adduct ion of MES
m/z	mass-to-charge ratio
P	pressure
PDO	2,4-pentanedione
$(PDO)NH_4^+$	ammoniated monomer ion of PDO
$(PDO)_2NH_4^+$	ammoniated dimer ion of PDO
R^2	regression coefficient
T	temperature
t_d	ion drift time
TEPO	triethyl phosphate
$(TEPO)H^+$	protonated monomer ion of TEPO
$(TEPO)_2H^+$	proton-bound dimer ion of TEPO

$(TEPO)NH_4^+$	ammoniated monomer ion of TEPO
$(TEPO)_2NH_4^+$	ammonium-bound dimer ion of TEPO
TOFMS	time-of-flight mass spectrometer
V	voltage

DISTRIBUTION LIST

The following individuals and organizations were provided with one Adobe portable document format (pdf) electronic version of this report:

U.S. Combat Capabilities Development
Command Chemical Biological Center
(CCDC CBC)
FCDD-CBR-ID
ATTN: Hauck, B.
McHugh, V.
Wade, M.

CCDC CBC
Technical Library
FCDD-CBR-L
ATTN: Foppiano, S.
Stein, J.

Joint Project Manager for Chemical,
Biological, Radiological and Nuclear Sensors
(JPM CBRN Sensors)
ATTN: Gauani, H.
Powers, M.
Matz, C.

U.S. ARMY COMBAT CAPABILITIES DEVELOPMENT COMMAND
CHEMICAL BIOLOGICAL CENTER